Volna−3 Doppler sodar

V.A. Gladkikh, A.E. Makienko, and V.A. Fedorov

Institute of Atmospheric Optics,
Siberian Branch of the Russian Academy of Sciences, Tomsk
Received December 30, 1998

A new three-channel monostatic Doppler sodar is described. The sodar is designed for remote measurements of the wind velocity profile and structure constant of temperature fluctuations, as well as for detecting temperature stratification of the boundary atmospheric layer. The Volna−3 sodar includes a minimum set of analog electronic blocks, which only provide for emission, reception, and pre-filtration of acoustic signals. Another its feature is digital conversion of a high-frequency acoustic signal into an equivalent low-frequency complex form. The information processing algorithms developed allow real-time measurements to be conducted without the use of specialized computer devices.

The Volna−3 three-channel Doppler sodar is designed to measure the wind velocity profile and the temperature structure parameter C_T^2, as well as to detect temperature stratification of the boundary atmospheric layer. Each channel of the sodar operates in the sequential monostatic pulsed mode thus providing for reception and processing of echo signals in real time. The sodar was designed taking into account the experience gained at exploitation of Zvuk−2 sodar,[1] so it can be considered as an upgrade of the latter achieved by elimination of some of its drawbacks. The basic drawbacks of Zvuk−2 sodar are low power of echo signals at nearly neutral thermal stratification of the atmosphere, insufficient noise protection under severe noise conditions, and the lack of a possibility of changing sodar parameters when determining the above-listed atmospheric characteristics.

The Volna−3 sodar includes three parabolic antennas and a minimum set of analog electronic blocks, which only provide for emission, reception, and pre-filtration of the acoustic signals. The analog blocks includes an amplifier of output signals, an echo pre-amplifier, a bandpass pre-filter, and a reception/transmission switch. Such a set is traditional, for sodars currently in use throughout the world (see, for example, Ref. 2), therefore its description is omitted in this paper. Much of the sodar functions (including initial generation of emitted pulses) are done in digital (discrete) form. One of the central parts of the sodar is a personal computer (IBM PC AT 386 or later modifications), which controls operation of the system as a whole. To do this, the computer is complemented with a controller. The controller operates by interruptions and includes an ADC, DAC, analog input, digital and analog outputs. The sodar is synchronized from the ADC digital outputs. First, a sonic pulse to be sent into the atmosphere is generated by the program. The operating frequency f_p is invariable in this modification of the sodar and equal to 1700.68 Hz, while the pulse duration τ_p is changeable and may be equal to 0.075, 0.15, or 0.3 s. The Tucky weighting function, which is well-known in the spectral analysis, is used as an envelope. It provides a certain compromise between the undesired decrease in the power of a sounding pulse (because of the necessity to reduce its edge values to zero) and useful suppression of side lobes in its power spectrum (spectral density). Numerical simulation of a sounding pulse in a digital form becomes, in this case, less computationally expensive. Then the digitally formed sounding pulse is converted into an analog signal with a DAC. The analog signal is amplified and directed through the reception/transmission switch controlled by the ADC controller digital outputs to the sodar antenna for further emission into the atmosphere. The echo signal is digitized by interruptions of the controller from a built-in timer with the discretization frequency $f_e = 4f_p = 6802.72$ Hz (for the 12-bit ADC).

The use of sounding pulses of different duration allows us to change the minimum altitude, from which the meteorological parameters can be determined, h_{min} (the "blind zone" of the sodar), the maximum altitude h_{max}, and the standard spatial resolution Δh_{st}. Thus, at $\tau_p = 0.075$ s, and allowing for some internal time delays that improve the performance of the Volna−3 sodar, $h_{min} \approx 22$ m, $\Delta h_{st} \approx 12.5$ m; at $\tau_p = 0.15$ s $h_{min} \approx 40$ m, $\Delta h_{st} \approx 25$ m; at $\tau_p = 0.3$ s $h_{min} \approx 80$ m, $\Delta h_{st} \approx 50$ m. The pulse with $\tau_p = 0.075$ s is usually used to study the lower atmospheric layer, while the pulse with $\tau_p = 0.3$ s is used to achieve the maximum sounding altitude. However, most drastic improvement of the sodar energy parameters has been achieved by the use of a new acoustic transceiving system. It employs a new horn emitter attached to the paraboloid, which was used in Zvuk−1 sodars.[3] The design of the horn emitter has been specially developed for application in Volna−3 sodar. It is an accumulator of acoustic power from four 50-W electrodynamic converters (heads). The system is schematically shown in Fig. 1.
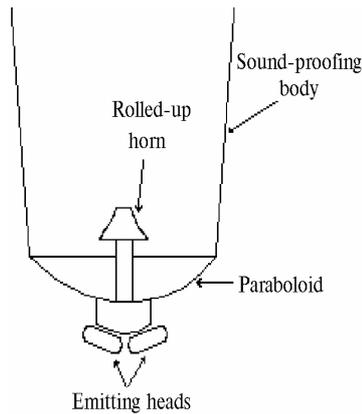
Fig. 1.

The use of a new emitter has allowed the sonic pressure of the emitted signal to be increased from 129.8 to 135.2 dB at the flare center of the sound-proofing cone. Besides, the use of the rolled-up horn has allowed the emitting heads to be set at the back side of the paraboloid, what makes the antenna maintenance more convenient. For the sake of comparison, Fig. 2 demonstrates records of echo amplitude obtained with the sodar employing different antennas of the Zvuk−2 and Volna−3 sodars. The ordinate is the altitude (in meters) the echo signal comes from. The signal amplitude is proportional to the degree of blackening on the plot. The time domains marked with 1 and 2, on the abscissa, show the signals acquired with the antenna of Volna−3 sodar and Zvuk−2 sodar, respectively.
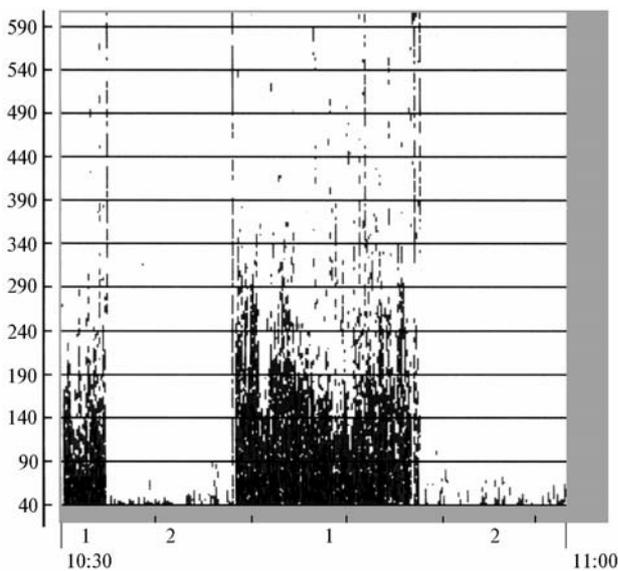
Fig. 2.

Figure 2 illustrates the difference between the maximum achievable sounding altitudes h_{max} of the sodars in this experiment. So, the maximum achievable altitude h_{max} in the mode of wind velocity measurements is increased from $50 - 60$ m, on the average, to 250 m. This difference can vary significantly

because it also depends on the state of the atmosphere. However, the gain from the use of the new transceiving system is quite obvious.

Let us give a more detailed description of the signal processing system of Volna−3 sodar since it differs significantly from the processing systems used in other sodars. Its salient feature is quadrature demodulation, that is, conversion of the received high-frequency acoustic signal into the low-frequency complex form. An advantage of the quadrature presentation of high-frequency signals is the following. This presentation enables faster post-detection processing, simplifies further amplitude-frequency demodulation, and facilitates different spectral transformations and synthesis of digital filters with symmetrical frequency characteristics. Besides, to increase the accuracy of conversion of the initial signal into the equivalent low-frequency presentation, it is worth performing the quadrature demodulation in the digital part of the receiving system rather than in the analog one. This is explained by identity of characteristics of the digital quadrature channels. Other factors in favor of this choice are the absence of influence of the zero drift and direct passage of control signals, as well as lower noise and smaller linear distortions. However, in this case it becomes urgent to speed up the above conversions. If the received signals are sufficiently narrow-band, this can be achieved by using lower frequencies of subdiscretization and further decimation (thinning out) of the processed signals.[4]

The Volna−3 sodar employs a complex demodulation by the delay method with a linear interpolation.[5] The idea of this method is rather simple. Assume that at the output of a sodar's band-pass filter we have an additive mixture of the narrow-band signal $u(t)$ and noise $n(t)$, which can be written in the following form

$$u(t) = U(t) \cos [2\pi f_e t + \varphi_e(t)] ,$$

$$n(t) = N(t) \cos [2\pi f_p t + \varphi_n(t)] ,$$

where $U(t)$ and $N(t)$ are the envelopes; $\varphi_e(t)$ and $\varphi_n(t)$ are random phases of the echo signal and noise; f_e is the mean frequency of the echo signal. Then the frequency oscillation $y(t) = u(t) + n(t)$ can be presented with low-frequency quadrature components of the mixture of the signal and noise $Y_c(t)$ and $Y_s(t)$ with respect to the reference frequency of the emitted pulse f_p:

$$y(t) = Y_c(t) \cos 2\pi f_p t - Y_s(t) \sin 2\pi f_p t , \quad (1)$$

where $Y_c(t) = U_c(t) + N_c(t)$, $Y_s(t) = U_s(t) + N_s(t)$, and $U_c(t) = U(t) \cos \theta(t)$, $U_s(t) = U(t) \sin \theta(t)$, $N_c(t) = N(t) \cos \varphi_n(t)$, $N_s(t) = N(t) \sin \varphi_n(t)$ are individual quadrature components of the signal and noise; $\theta(t) = 2\pi f_d t + \varphi_e(t)$, $f_d = f_e - f_p$ is the Doppler shift of the echo frequency with respect to f_p. In this case the complex envelope $Z(t) = Y_c(t) + jY_s(t)$.

Assume that the frequency of discretization of the processed high-frequency process $f_s = 1/\Delta t = 4f_p$, and the discretization interval of the quadrature components ΔT is equal to $4\Delta t$, that is, $\Delta T = 4\Delta t\, m = M\Delta t$, where $M = 4m$ is the coefficient of decimation of readouts of the low-frequency quadrature components with respect to the initial high-frequency sample $y(n\Delta t)$, $m = 1, 2, ..., m_{max}$. The maximum M depends on the width of the oscillation spectrum of $y(t)$. Let us consider certain moment in time, t_0, which satisfies the condition $t_0 = n\Delta T$, where n is the integer number. Then $y(t_0) = Y_c(t_0)$, $y(t_0 - \Delta t) = Y_s(t_0 - \Delta t)$, and $y(t_0 + \Delta t) = -Y_s(t_0 + \Delta t)$ according to Eq. (1). Thus, the readouts of the high-frequency oscillation separated by $\Delta t = 1/4f_p$ coincide with the corresponding readouts of the low-frequency quadrature components ($y(t_0 + \Delta t)$ accurate to sign). Thus obtained quadrature components correspond to different moments in time; they are shifted by Δt with respect to each other. Taking into account that they vary slowly during Δt, the usual linear interpolation can be applied to the second quadrature component. As a result, we obtain simple estimates for the quadrature components and complex envelope from the readouts of the highest-frequency oscillation:

$$\begin{cases} \hat{Y}_c(n\Delta T) = y(n\Delta T), \\ \hat{Y}_s(n\Delta T) = [y(n\Delta T - \Delta t) - y(n\Delta T + \Delta t)]/2, \quad (2) \\ \hat{Z}(n\Delta T) = \hat{Y}_c(n\Delta T) + j\hat{Y}_s(n\Delta T), \end{cases}$$

where $n = 0, 1, ..., N_q - 1$, $N_q = [(N - 1)/M] + 1$ is the number of readouts of the quadrature components resulting from N readouts of the initial signal with the coefficient of decimation M; [   ] denote the integer part of a number.

The accuracy characteristics of the "quadraturization" (2) depend mainly on the band narrowness (characterized by $y(t)$) and the relative value of the Doppler shift f_d/f_p (Ref. 5). For broadband signals the estimates by Eq. (2) cannot be used because in this case they are characterized by intolerably large errors. The criteria presented in Ref. 5 were used as a basis for theoretical evaluation of the possibility to use algorithm (2) in the problems of acoustic sounding of the atmosphere. In this evaluation we used the system and signal parameters and Doppler shifts that are typical of the case considered here. As a result, we have concluded that "quadraturization" (2) can be used in meteorological sodars provided that the high-quality bandpass pre-filtration is used.

Figure 3 shows the structure scheme of processing for the vertical channel of the Volna–3 sodar, and Fig. 4 shows in detail the relations characterizing the process of the quadrature demodulation for one processed gate of the echo from the altitude of 220 m at $\tau_p = 0.15$ s. (As an analog pre-filter, to decrease the dynamic range of the processed signals and to ensure correct operation of the digital devices, the Volna–3 sodar employs an active bandpass filter with the cut-off frequency of (1700.68 ± 135) Hz at the half-power level.) The measurements were conducted in the urban area, so they were accompanied by strong industrial noise at the frequency near 1830 Hz. The analog filter failed to suppress this noise. The Doppler signal was also observed against the background of this noise.
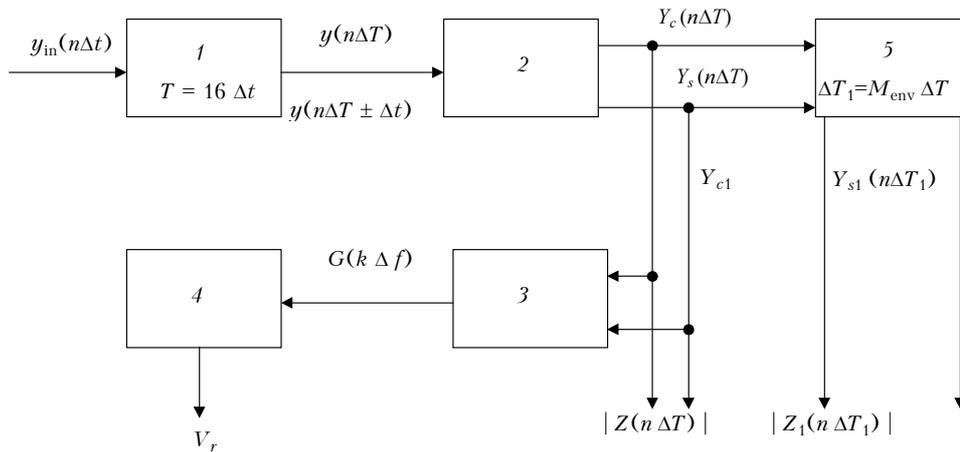
Fig. 3. The structure scheme of processing for the vertical channel of the sodar: the Butterworth band-pass filter of the 8th order with the cut-off frequency of 1700.68±50 Hz (*1*); the unit for quadrature demodulation (*2*); the unit for spectral analysis (*3*); the unit for calculation of the radial wind velocity (*4*); the low-frequency quadrature Butterworth filter of the 4th order (*5*).

Figure *4a* well illustrates this situation. The ordinate shows the obtained values of power of the input signal $y_{in}(n\Delta t)$(in ADC readouts). After the ADC the signal $y_{in}(n\Delta t)$ enters the input of the discrete bandpass Butterworth filter of the 8th order.[6] The signal

has the central frequency $f_p = 1700.68$ Hz and the width of 100 Hz at the level of 0.707 (see Fig. 3, unit *1*). This allows us to measure the vertical wind velocity ranging within ± 4 m/s. The amplitude–frequency and phase–frequency characteristics of the filter from the

frequency of 0 Hz to the Nyquist frequency $f_N = f_s/2 = 3401.36$ Hz are shown in Figs. 4b and c. The industrial noise is almost fully suppressed at the output of the filter (Fig. 4d). In connection with a wide use of different digital (discrete) filters in the Volna−3 sodar, note the necessity of allowing for their dispersive action upon the processed signals. The Butterworth filters are used because they possess maximally flat amplitude−frequency characteristics and sufficiently linear phase−frequency characteristics $\varphi(f)$ in the pass bands along with a high speed of operation. Thus, in spite of the generally nonlinear behavior of $\varphi(f)$ shown in Fig. 4c, in the pass band it can be approximated by the linear dependence $\varphi(f) = 4866.184 - 2.86125\,f$, what results in a practically constant characteristic of the group delay in the range considered. Specifically, we can say that this filter, along with the frequency conversion, simply delays the processed echoes by 54 intervals of

discretization Δt without additional distortions. Note that each of the discrete filters used in the sodar is characterized by not only its time delay but also by the setting time. This fact was also taken into account when developing the processing program for the sodar.

Then the filtered signal enters the quadrature modulation unit 2. Here the quadrature components $Y_c(n\Delta T)$ and $Y_s(n\Delta T)$ are generated with the coefficient of decimation M in accordance with Eq. (2). Let us consider the choice of the coefficient M. From the viewpoint of the discrete Fourier transforms, realization of Eq. (2) involves "multiplication" of the initial high-frequency signal $y(t)$ along the frequency axis of the narrow-band power spectrum $G(f)$ with the period $f_{s,q} = f_s/M$ Hz. The frequency of the emitted pulse f_p is transferred in one of the "multipliedB lobes exactly to the zero frequency. (Further just this lobe is processed because it corresponds to the spectrum of the complex envelope in its principal Nyquist band.)

a

b
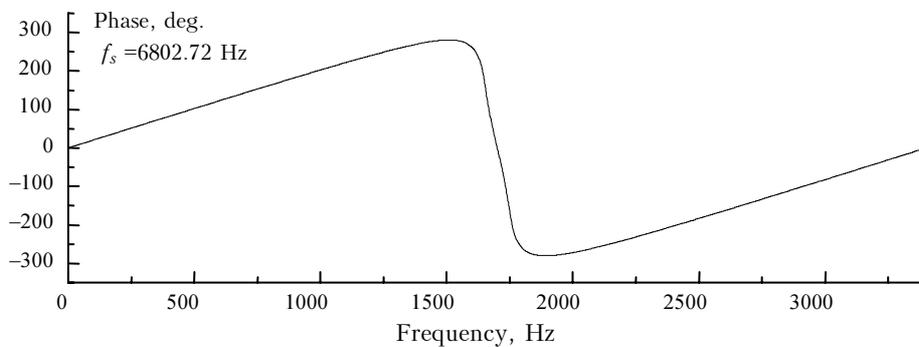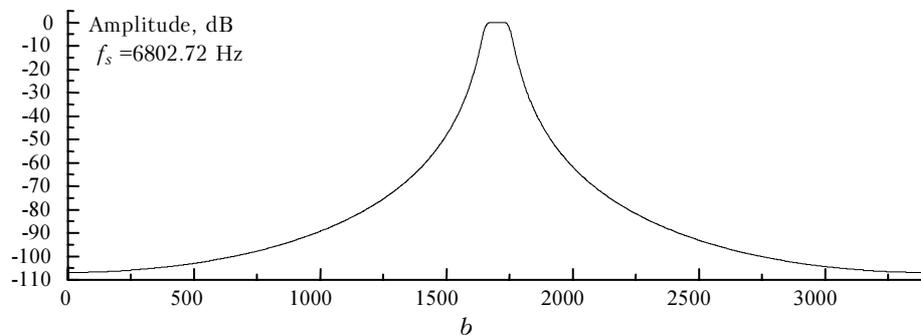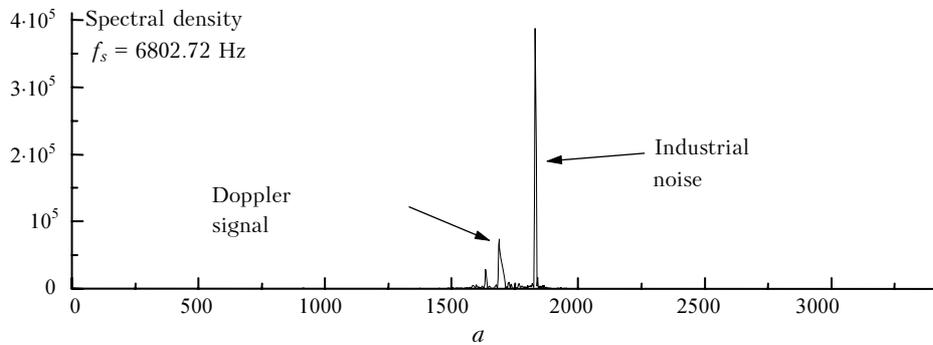
c
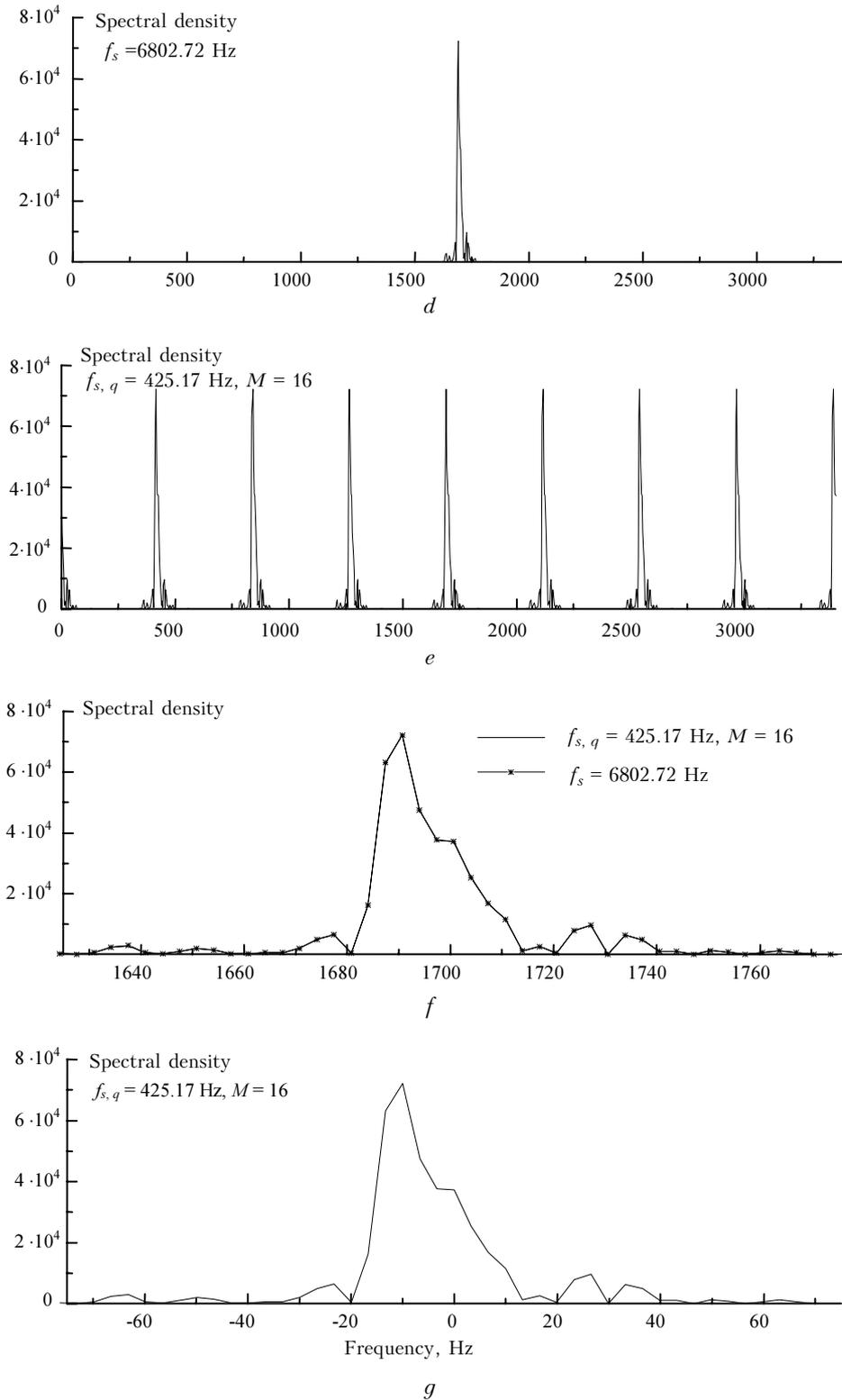
Fig. 4. Power spectra recorded within a single range gate at the altitude h = 220 m: high-frequency acoustic echo signal after input analog filtration (f_s = 6802.72 Hz, sample size N = 1024 real readouts) (*a*); echo signal at the output of the band-pass Butterworth filter (f_s = 6802.72 Hz, N = 1024) (*d*); the complex envelope obtained with the decimation coefficient M = 16 in the positive section of the Nyquist region of the high-frequency echo signal ($f_{s,q}$ = 425.17 Hz, the sample size N_q = 64 complex readouts) (*e*); comparison of the versions *d* and *e* in the significant band of the initial echo signal (*f*); the complex envelope in the significant area of its principal Nyquist region (*g*); the amplitude-frequency characteristic of the digital band-pass Butterworth filter of the 8th order with the central frequency at 1700.68 Hz and bandwidth of 100 Hz (*b*); the phase-frequency characteristic of the filter (*c*).

To exclude overlapping, that is, influence of lobes on each other, the coefficient M should fit the significant frequency spectral band $G(f)$, which is formed by the pass band of the discrete filter (see Fig. 3, unit 1). For this to take place, it is sufficient to require that $f_{s,q} \geq \Delta f_f$, where Δf_f is the filter bandwidth at the level of -40 dB. In this case $\Delta f_f = 318$ Hz, what leads to the requirement that $M \leq 21$. We have selected $M = 16$, what almost completely excludes spectral overlapping. All the above-said is illustrated by Figs. $4d-g$. Note that almost complete coincidence occurs of the spectra of a gate at the reference high-frequency processing ($f_s = 6802.72$ Hz) with the obtained complex envelope ($f_{s,q} = 425.17$ Hz). This coincidence confirms the applicability of this method of quadrature demodulation. The algorithm (2) was also checked at the coefficients of decimation $M > 16$. At $M \leq 32$ we did not observe some significant errors in "quadraturization.B Catastrophic errors appeared only at $M \geq 60$.

Because the algorithm (2) is simple, it is possible to combine the process of filtration and obtaining of the quadrature components with the required coefficient of decimation M. In this case the input readouts of the echo signal $y_{in}(n\Delta t)$ are filtered as they come, but only three neighboring output signals are gated with the step M accompanied by simultaneous formation of the quadrature components. Thus, at the filter output we have the sequence of readouts of the low-frequency complex envelope $Z(n\Delta T) = = Y_c(n\Delta T) + jY_s(n\Delta T)$ of the processed high-frequency signal $y(n\Delta t)$. This algorithm is implemented in the ASSEMBLER program thus allowing almost real-time processing of the echoes.

Then the quadrature components $Y_c(n\Delta T)$ and $Y_s(n\Delta T)$ in unit 3 (see Fig. 3) are gated by the number of readouts agreed with the duration of the emitted pulse τ_p and are subjected to spectral processing in the band from -45 to $+45$ Hz with the step $\Delta f = 1/2\tau_p$ (in Hz). Then they are smoothed by a sliding average. As follows from the above-said, the obtained spectrum of the complex envelope is the Doppler spectrum of the echo signal. For interpolation of the wind data, the procedure of "jumpingB spectral analysis (with overlapping of the processing gates) is used. To make measurements more flexible without loss in speed, we have refused from using of the fast Fourier transform algorithm in favor of the spectral algorithm, which we have specially developed. It involves recursion calculation of the trigonometric functions taking into account the symmetry of the used frequency grid about $f = 0$ Hz. Then unit 4 performs the initial search of the position of the maximum of the smoothed spectrum f_{max}. Simultaneously, the second (in significance) spectral maximum is sought outside the frequency band occupied by the main peak. Then the power of the signal and noise and the signal-to-noise ratio are calculated in the equivalent bands. The signal-to-noise ratio is then compared with the threshold q

preset by an operator. As the threshold is exceeded, to refine f_{max}, the parabolic approximation of the main spectral peak is made followed by calculation of the radial wind velocity V_r in the   volume gated. Otherwise, V_r is not calculated. We can say that V_r is determined at large q only in the presence of pronounced signal peaks, that is, when measurements are characterized by high reliability. At smaller q the reliability of the results decreases, what should be compensated for by further processing.

The complex envelope $Z(n\Delta T)$ is also used for obtaining the readouts of the envelope of the echo signal at the emitted pulse frequencies proportional to C_T^2. Toward this end, the readouts of $Z(n\Delta T)$ are filtered with a two-channel quadrature low-frequency Butterworth filter of the fourth order (unit 5). To increase the flexibility of the acoustic sounding of the thermal structure of the atmosphere, different cut-off frequencies of the filter can be used, namely, ± 4.25, ± 8.5, ± 17 Hz. Besides, depending on the maximum sounding altitude and some other factors, we apply different coefficients of decimation of the envelope M_{env} of the output readouts $Z_1(n\Delta T_1) = Y_{c1}(n\Delta T_1) + + jY_{s1}(n\Delta T_1)$, where $\Delta T_1 = M_{env} T$. The readouts of the sought envelope, i.e., $|Z_1(n\Delta T_1)|$ are determined from the found values of $Z_1(n\Delta T_1)$.

Upon completion of the processing for the vertical channel, the system automatically starts the cycle of sending, reception, and processing of information from the slant sounding channels. In contrast to the vertical channel, they do not include quadrature low-frequency filters. So there is no need in calculation of the corresponding envelope. The parameter V_r is measured similarly to the above-described procedure. However, because of a wide range of Doppler velocities, the band-pass Butterworth filter of the 8th order with the bandwidth of 200 Hz is applied, and the coefficient of decimation $M = 8$. Spectra of complex envelopes are calculated from -95 to $+95$ Hz.

Upon completion of the given measurement cycle, the altitude profile of the mean wind velocity vector $\mathbf{V}(h)$ is calculated taking into account the sounding geometry, which may vary depending on the measurement site. To automatically compensate for contribution from possible anomalous errors in measurement of radial wind velocities $\mathbf{V}_{r,i}(h)$ into $\mathbf{V}(h)$, we first apply the following procedure. For every altitude gate, the variational series of obtained instantaneous values of the wind velocity $\mathbf{V}_{r,i}(h)$ is constructed. Here $i = 1, 2, ..., N_{soun}$, N_{soun} is the number of sounding cycles, for which the parameter $\mathbf{V}(h)$ is calculated. This series is used to obtain five estimates of primary mean values: sample-size mean, sample mean over the entire sample, sample mean with rejection of 50% of extreme values, median, and quartile mean of the sample. Then the median of the above-listed five means is taken as the mean value sought, which is then used in calculation of $\mathbf{V}(h)$. Use of this procedure is worthwhile even in the absence of

anomalous errors in measurement of the radial wind velocities, because it allows more correct determination of the centers of their distributions. The traditionally used estimate of the center as a sample mean is efficient only for distributions close to the normal one. For other types of distributions it may be rather bad.

To check functioning of the instrumentation and to estimate the sounding altitude h_{max}, the sodar is started in the test mode prior to the main measurement cycle. In the test mode, the computer monitor displays the received acoustic signals and their averaged power spectra of all range gates for the preset number of sounding cycles. The knowledge of actual h_{max} corresponding to specific meteorological conditions allows the acoustic signals to be received and processed only up to this altitude. Thus, the further measurement process can be optimized from the viewpoint of spatiotemporal selection and processing of information. In our previous Zvuk−2 sodar, the altitude h_{max} was constant (500 m). As a result, unreliable information was often received and processed. Thus, the extended duration of sounding cycles was unjustified, and the reliability of results was low even at the altitudes, the echo signal from which had sufficiently high power.

The operation of the Volna−3 sodar is also continuously checked during the measurement process by displaying the envelopes of the currently processed acoustic signals (having passed through the corresponding band-pass filters). For the vertical channel, the envelope of the signal having passed through the quadrature filter is displayed as well.

Figure 5 shows the information, which is displayed on the computer monitor during the measurements. At the upper left panel the facsimile record for the earlier 30 min of the operation of the vertical channel is continuously displayed. The envelope of the echo signal of the second channel obtained in the current sounding cycle is shown in the right panel (the antenna of the second channel is inclined at 20° to the vertical). The Table of the wind data averaged for the previous 10-minute measurement cycle is shown at the upper right. The mean vertical profile of the horizontal wind velocity is shown separately at the bottom. The missing data in some cells of the Table correspond to unreliable results by the criterion of preset signal-to-noise ratio $q = 4$. At the lower left the monitor displays the information about data recording into the corresponding files.

Institute of Atmospheric Optics. Atmospheric Acoustic Lab. 4 cycles. Date: 10.14.98. 11:53

Altitude, m	Vertical wind	Radial 1	Radial 2	Horizontal wind	Direction
52	−0.41	−1.53	0.39	4.05	325.8
72	−0.26	−1.19	0.92	4.38	308.7
92	−0.38	−2.42	1.13	7.43	324.3
112	−0.50	−2.92	1.38	8.98	322.9
132	−0.38	−3.13	0.90	8.91	335.8
152	−0.43	−2.70	0.69	7.44	334.4
172	−0.48	−2.96	1.17	8.74	327.0
192	−0.58	−2.97	0.79	8.10	331.2
212	−0.12	−2.66	0.80	7.90	340.4
231	−0.33	−2.54	2.01	9.41	313.7
252	0.17	−3.80	1.87	12.60	336.6
272	−0.36	−2.89	2.05	10.23	317.0
292	0.02	−4.48	1.04	13.49	347.2
312	−0.11	−5.10	1.80	15.64	339.1
332	0.15	−4.96	2.14	16.02	338.6
352	0.12	−5.32	1.32	16.27	347.5
372	0.15	−4.41	3.07	15.83	327.3
392	0.11	−4.23	2.55	14.57	330.6
412	0.28	−4.17	2.67	14.74	331.5
432	−0.21	−5.22	1.33	15.35	343.1
452	0.32		3.25		
472		−4.91	2.80		
492		−4.73	0.81		
512		−1.67	0.72		

2nd channel

Criterion of information recordind in a file

■ facsimile signal

■ mean wind

■ instantaneous wind

Fig. 5.

Besides the program developed to control the sodar operation and to display the parameters during measurements, we have developed additional utilities for secondary processing of the data obtained. Among these utilities there are, in particular, the following programs: 1) the browser for facsimile records (these files have unique format, so they need a special browser to be viewed); 2) the program for presentation of the wind data in both the tabulated and graphical forms (by wind direction and wind speed). Both utilities allow scrolling of the displayed information (along the time scale), what is especially important for long measurements. All the programs for operation of the sodar are integrated within the same shell, what provides for their convenient and efficient use. Both MS–DOS and MS–WINDOWS versions are available. For the MS-DOS version we used Borland C++ language for the programs (and Turbo Vision for the shell); in the WINDOWS version the programming language was Borland Delphi. The WINDOWS operating system allows development of more convenient and easy-to-use applications, which can be easily complemented with new functional capabilities or changed if necessary. Besides, the WINDOWS operating system allows the maximum use of the system resources (in particular, RAM) when operating in Safe mode.

The algorithms and software developed provide the capability to measure altitude profiles of the wind velocity and amplitudes of the echoes in real time without specialized computer devices. At the same time, all currently existing real-time sodars, which involve spectral processing at the initial frequency, have to use powerful specialized processors (see, for example, Ref. 2). Note also that the quadrature demodulation implemented in the Volna–3 sodar allows the amplitude and phase–frequency modulation of received acoustic signals to be studied correctly. This fact will allow further increase in the information content and reliability of sounding. In the near future the sodar will be improved to enhance its noise immunity and flexibility of control and to extend its functional capabilities.

Acknowledgments

References

1. V.A. Gladkikh, N.P. Krasnenko, and V.A. Fedorov, in: *Extended Abstracts of COST-76 Profiler Workshop 1997,* Engelberg (1997), Vol. 1, pp. 174–177.
2. *AR - 410 Doppler Sodar. Booklet of KAIJO CORPORATION*, Catalog No. M-441-21E. Tokyo, Japan.
3. V.A. Gladkikh, V.I. Karpov, et al., Atmos. Oceanic Opt. **5**, No. 7, 473–477 (1992).
4. N.P. Krasnenko and V.A. Fedorov, in: *Extended Abstracts of COST-76 Profiler Workshop 1997,* Engelberg (1997), Vol. 1, pp. 182–185.
5. V.A. Fedorov, Avtometriya, No. 4, 110–114 (1994).
6. L. Rabiner and B. Gold, *Theory and Application of Digital Signal Processing* [Russian translation] (Mir, Moscow, 1978), 848 pp.